Dynamic and Debye Shielding and Antishielding in Magnetized, Collisionless Plasmas

C. Hansen and J. Fajans
Physics Department, University of California, Berkeley, Berkeley, California 94720-7300
(Received 23 November 1994)

While shielding in *collisional*, strongly magnetized (one-dimensional) plasmas obeys the standard Debye result, shielding in *collisionless*, immobile ion plasmas is far more complex than commonly believed. In some circumstances, the plasma will *antishield* a positive test charge; i.e., the plasma becomes more *positive* in the neighborhood of a positive test charge. When shielding does occur, it results solely from electrons dynamically trapped in the neighborhood of the test charge. The new theory of dynamic shielding, developed herein, is in good agreement with experiments in pure electron plasmas.

PACS numbers: 52.25.Mg, 52.25.Kn, 52.25.Wz, 52.35.Sb

Collisionless shielding in one-dimensional (highly magnetized) immobile ion plasmas is paradoxical. The insertion of a positive test charge into such a plasma locally accelerates the plasma electrons, causing them to move faster in the vicinity of the test charge. Since flux conservation requires that faster moving electrons have lower density, the density of the negatively charged electrons will *decrease* around the test charge [1]. The plasma *antishields* the test charge; instead of decreasing the net positive charge near the test particle, the plasma will *increase* the net charge. This phenomenon has been sporadically recognized in the literature [2–6], but, to our knowledge, has never before been observed.

Although we observe antishielding when we employ unusual initial conditions, more commonly we observe the converse—shielding. We show here that this shielding results from the presence of electrons trapped in the potential well of the test charge. While several different mechanisms can trap electrons, a ubiquitous, fast acting, transit-time mechanism always traps electrons when the test charge is introduced adiabatically [7]. That one-dimensional (1D) collisionless shielding requires trapping does not appear to have been previously recognized, and the explanation of shielding given in many textbooks and papers is incorrect or incomplete [2–5,8–10]. Because the trapping results from dynamic processes, we call the resulting shielding "dynamic" shielding. Both the observed and calculated magnitude of dynamic shielding can be significantly smaller than Debye shielding; eventually collisions transform the dynamic shielding to Debye shielding.

Shielding and antishielding are distinguished by their different phase space loading. As shown in Fig. 1, the phase space in the neighborhood of a positive potential test well contains two distinct classes of orbits: free orbits on which electrons stream through the well, and trapped orbits that close within the well. Since the phase space area filled by any given set of free electrons lengthens in $\hat{z}$ as the set accelerates into the test well, Liouville's theorem requires that the $\hat{v}_z$ extent shortens concomitantly. In steady state, the phase space density distribution function $f(z, v_z)$ must be constant along any trajectory. Consequently, the electron density $n(z) = \int f(z, v_z)\, dv_z$ must decrease inside the test well if the trapped orbits are unpopulated, and the well will be antishielded. Shielding (density increase), as is found for adiabatically created wells, can result only from the trapped orbits being populated.

The results we report were observed in a pure electron plasma held in a Penning-Malmberg trap (Fig. 2). The plasma in such traps lies along the common axis of a series of collimated, cylindrical ($r = 1.905\,\mathrm{cm}$) electrodes. The electrodes are biased to create an electrostatic well, thereby providing axial confinement. A strong axial magnetic field (1800 G) provides radial confinement, and also ensures that the electron motion is one dimensional. More detailed descriptions of Penning-Malmberg traps can be found in the literature [11].

We create the equivalent of a positive test charge by biasing a central electrode to create a square, secondary, positive electrostatic test well (see Fig. 3). The manner in which the test well is created determines the plasma response; when the test well is created nonadiabatically the plasma enhances (antishields) the test well depth, but

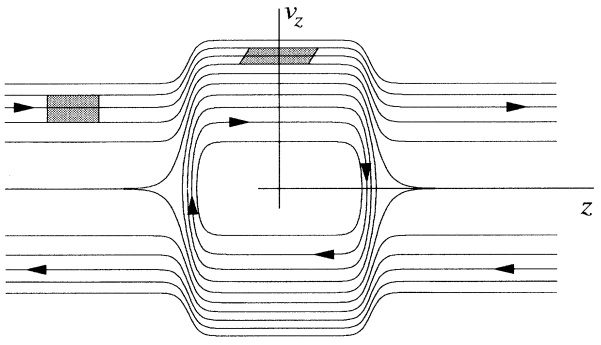

FIG. 1. Electron orbit phase space in the vicinity of a positive test well. Note the change in aspect of the square set of electrons as they propagate into the well.

0031-9007/95/74(21)/4209(4)$06.00

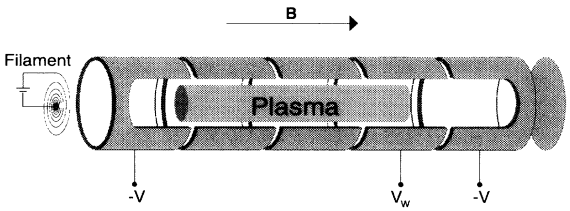

FIG. 2. Schematic of the experiment with a cutaway to show the plasma. Each cylinder is separately biasable.

when the test well is created adiabatically the plasma diminishes (shields) the test well depth. We generate nonadiabatically created test wells (non-ACTW) by allowing the plasma to flood into a region in which the test well is already present. Under these conditions the electrons encounter the test well on a time scale comparable to their axial bounce time (0.1 μs). Adiabatically-created test wells (ACTW) are generated by slowly ramping (10 μs) the test well depth from zero to its final value with the plasma already present in the test well region. The final plasma radius is approximately 1 cm, the final density is $n_0 \approx 1.2 \times 10^7\{\mathrm{cm}^{-3}\}$, and the plasma temperature is 6.8 eV.

The total charge, and thus the number of electrons contained within the test well, equals the image charge on the test well electrode, and is measured by integrating the image current which flows onto the test well electrode. Figure 4 shows this total charge as a function of the test well depth. The total charge in the test well increases with test well depth for the adiabatically created test well, but it decreases for the nonadiabatically created test well. Hence the test well is shielded in the first case and antishielded in the second.

When the right wall of the overall confinement well is removed (step 5 in Fig. 3), electrons not trapped in the test well are no longer confined and stream out along the magnetic field lines. When the test well potential itself is removed, the trapped electrons are also released, and this trapped charge can be measured by monitoring the test well electrode image current. Because of changes in the self-consistent response of the plasma itself, the trapped charge that remains after the free charge escapes is not precisely equal to the trapped charge when the free charge is also present. As shown in Fig. 4, the trapped charge increases linearly with test well depth for shallow, adiabatically created test wells. In contrast, little charge is trapped by shallow nonadiabatically created test wells. All measurements were made within 1 ms of step 3 (see Fig. 3). (Note that Fig. 4 shows the initial trapped charge; irregular instabilities are present in the nonadiabatic case that trap electrons. The onset of these instabilities occurs more rapidly as the test well depth is increased, and interferes with our nonadiabatically created well measurements for well depths greater than ten volts. The instabilities also prevent us from analytically predicting the nonadiabatic response.)

When the test wells are adiabatically created, electrons are efficiently and automatically trapped by a transit time mechanism. The mechanism is discussed by Lifshitz and Pitaevskii [7]: Consider a slow-moving electron entering a slowly deepening test well. Although the electron gains kinetic energy while entering the test well and loses kinetic energy while climbing out of the test well,

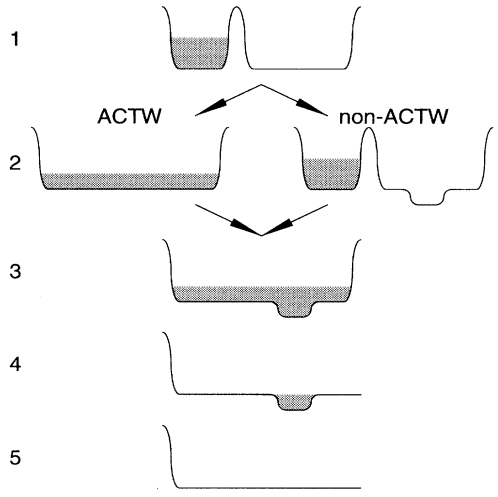

FIG. 3. Test well creation schemes. For clarity, the potentials are inverted. Step 1: Trap the initial plasma. Step 2: Adiabatic case (ACTW)—flood the plasma into the entire trapping region. Step 2: Nonadiabatic case (non-ACTW)—form the well. Step 3: ACTW—form the well and non-ACTW—flood the plasma into the entire trapping region. Step 4: Release and measure the image charge of the untrapped plasma. Step 5: Release and measure the image charge of the plasma trapped in the test well. The initial plasma length (step 1) is 12.8 cm, the final total plasma length is 29.3 cm, and the test well length is 11.5 cm.

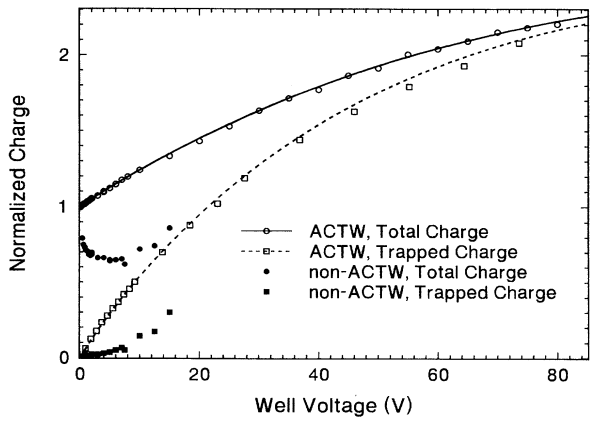

FIG. 4. Charge vs well voltage (depth). Measured values are indicated by the symbols, and the lines are calculated from the ACTW theory described in the text.

its kinetic energy remains constant inside the test well, even when the test well depth is varying. If during the electron transit time Δt the well depth has increased sufficiently, the electron will not be able to climb out of the well. Specifically, the electron will be trapped when $E_0 < e\Delta t\, d\Phi_w/dt$, where E_0 is the electron's initial kinetic energy outside the test well, e is the electron charge, and Φ_w is the effective test well depth. Since this mechanism is very general, it will occur regardless of whether the test charge is slowly increased in magnitude in place, or slowly introduced from outside the plasma.

The exact plasma response to an adiabatically created test well is most easily calculated with the use of the bounce adiabatic invariant $J = \oint v_z\, dz$, and relies on the fact that the initial velocity of each electron (v_0) is a constant of the motion for that electron. Consequently, the distribution functions inside and outside the test well are given by $f_w(v_w) = f_0[v_0(v_w, \Phi_w)]$ and $f_{\rm ext}(v_{\rm ext}) = f_0[v_0(v_{\rm ext}, \Phi_w)]$, respectively, where Φ_w is the well depth, v_w is the velocity in the well, $v_{\rm ext}$ is the velocity outside the well, and f_0 is the initial density distribution function. The densities inside $n_w(\Phi_w)$ and outside $n_{\rm ext}(\Phi_w)$ the well can be found by integrating the appropriate distribution functions.

The complete derivation of the plasma response is too long to be included here. However, it is easy to show that, to first order, the number of trapped electrons increases as $\sqrt{\Phi_w}$, where the square root reflects that the trapping depth is itself proportional to $\sqrt{\Phi_w}$. Consequently, trapping (and shielding) is inherently nonlinear, and there is no limit in which the trapped population can be ignored. However, to first order, the free population decreases as $\sqrt{\Phi_w}$. These two square root terms cancel, and it can be shown that the net density inside the well increases linearly [7] with Φ_w, namely, $n \approx n_0(1 + e\Phi_w/kT)$.

Calculation of the complete plasma response to an external potential is complicated by self-consistent effects. As the plasma density changes, it modifies the effective well depth. The self-consistent well depth $\Phi_w(V_w)$ can be found by solving the equation

$$\Phi_w(V_w) = V_w + \Phi_{p,\rm int}(\Phi_w) - \Phi_{p,\rm ext}(\Phi_w), \qquad (1)$$

where V_w is the externally applied test well depth, $\Phi_{p,\rm int}(\Phi_w)$ is the potential of the plasma residing inside the well, and $\Phi_{p,\rm ext}(\Phi_w)$ is the potential of the plasma residing outside the well. Thus $\Phi_{p,\rm int} - \Phi_{p,ext}$ is the potential drop across the well boundary resulting from the plasma itself. A more complete calculation of the self-consistent well depth would take into account the finite radial extent of the plasma; since the plasma radius is greater than a Debye length, the self-consistent response varies at different radial positions. Such three-dimensional effects (3D) are minimized in our plasma because the plasma radius is only 1.9 Debye lengths across, and we employ a response averaged over the observed radial profile in this paper. A more detailed study of 3D effects will be reported in a future paper.

The predicted charge inside the well $\mathcal{V} n_w[\Phi_w(V_w)]$ is graphed in Fig. 4 ($\mathcal{V}$ is the volume of plasma in the well). There are no fitted parameters in the theory. When the free charge is released, the self-consistent problem changes. The remaining trapped charge is found by solving the equation for the self-consistent well depth, $\Phi_T(V_w) = V_w + \Phi_{p,\rm int}(\Phi_T)$. The predicted trapped charge $\mathcal{V} n_T[\Phi_T(V_w)]$ is also graphed in Fig. 4. Note that the charge trapped before the release of the free electrons, $\mathcal{V} n_T[\Phi_w(V_w)]$, can be substantially greater than $\mathcal{V} n_T[\Phi_T(V_w)]$, and that self-consistent effects account for the linear rather than square root dependence of $n_T[\Phi_T(V_w)]$ on V_w.

Collisional processes eventually Maxwellian distribute the plasma, and the plasma equilibrium will gradually approach the standard Debye form. As shown in Fig. 5, plasmas subjected to both adiabatically and nonadiabatically created wells approach nearly the same final equilibrium, with the small differences in the final state likely due to differences in the final temperatures. The relaxation takes approximately 1 s, substantially longer than the collision time for the initial plasma. The slowness of the relaxation probably results from the high velocity of the free electrons while in the well; this high velocity reduces their collisional cross section. The gradual evolution that continues to beyond 10 s is due to global expansion of the plasma.

When Eq. (1) is linearized for small V_w, we find that the resulting density is

$$n_w = n_0(1 + eV_w/kT). \qquad (2)$$

This is identical to the density predicted by linearizing the Boltzmann relation $n_w = n_0 \exp(eV_w/kT)$. Because of this numeric coincidence, most results, including derivations of Debye shielding, that mistakenly or implicitly use the Boltzmann relation will still be correct in the collisionless regime. However, the Boltzmann result increases

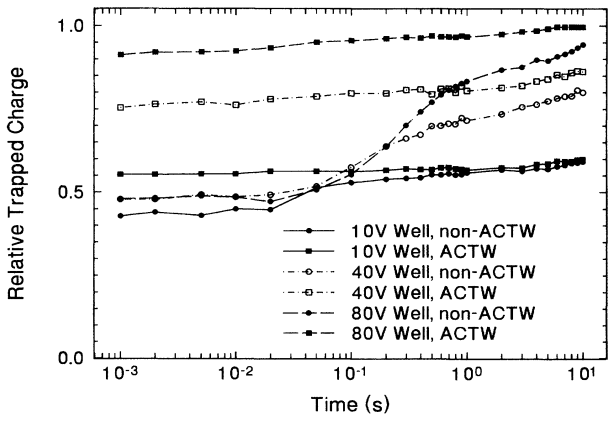

FIG. 5. Trapped charge normalized by total charge vs time for adiabatic and nonadiabatically created test wells, demonstrating the approach to equilibrium.

exponentially with V_w, while the numerically determined solution of Eq. 1 remains roughly linear. Thus nonlinear Boltzmann based, classic Debye shielding is stronger and more complete than transit-time trapping-based, dynamic shielding. As shown in Fig. 6, large exterior well voltages V_w are better shielded (larger perturbed density) as collisions change the response from the dynamic to the Debye shielding regimes. The Boltzmann theory curve shown in Fig. 6 is found by suitably modifying Eq. (1).

In conclusion, we have shown that collisionless shielding in one-dimensional plasmas relies on transit-time trapping. Without trapping, the plasma antishields a positive test charge. Since the electrons in highly magnetized plasmas respond one dimensionally, dynamic shielding is quite common.

The trapping mechanism discussed in this Letter also modifies the shielding response in two and three dimensions. For example, contrary to the result in the literature [6], collisionless plasmas shield line test charges.

We have assumed here that the plasma ions are immobile. If this assumption is relaxed, the ions will eventually respond to the test charge. Because very slowly moving ions will be entirely excluded from the region around the positive test charge, the response of the ions will follow the Boltzmann distribution [6].

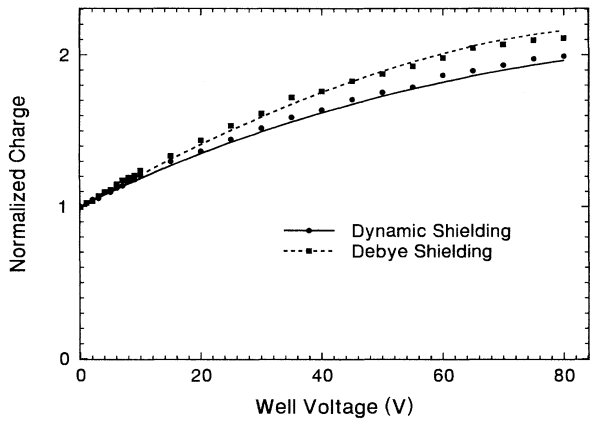

FIG. 6. Total charge vs well voltage. The "dynamic shielding" measurements were made immediately (1 ms) after the test well was adiabatically created, while the "Debye shielding" measurements were made after the plasma collisions were Maxwellian distributed, 1 s after the well was created. The lines are calculated from the theory described in the text.

Although the physics is different (still collisionless), the ions will shield the test charge in a manner akin to the standard Debye shielding result. Similarly, electrons will be excluded from the region around a negative test charge, and Debye-like shielding will result [6].

This work illustrates a problem by solving the Vlasov equation by linearization. Because the number of trapped particles scales as the square root of the perturbed potential, the number of these particles is not small [12]. The correct solution of the Vlasov equation requires that the number of trapped particles and the mechanism by which they are trapped be carefully considered. Where trapped particles are suppressed or otherwise controlled, such as for our nonadiabatically created wells, linearization of Vlasov's equation fails, and unusual phenomena like antishielding, double layers, and BGK modes occur.

We thank Dr. B. R. Beck, Dr. R. Gould, Dr. T. M. O'Neil, and Dr. J. S. Wurtele for their helpful comments. This work was supported by the Office of Naval Research.

[1] The paradox does not occur in two or three dimensions because the electron orbits bend.
[2] B. Abraham-Shrauner, Physica (Utrecht) **43**, 95 (1969).
[3] D. Montgomery and F. Tappert, Phys. Fluids **15**, 683 (1972).
[4] E. W. Laing and A. L. Gibson, J. Plasma Phys. **14**, 433 (1975).
[5] P. Chenevier, J. M. Doloique, and H. Peres, J. Plasma Phys. **10**, 185 (1973).
[6] N. M. Meyer-Vernet, Am. J. Phys. **61**, 249 (1993).
[7] E. Lifshitz and L. Pitaevskii, *Physical Kinetics* (Pergamon Press Inc., New York, 1981), p. 146; the authors include an untraceable reference to A.V. Gurevich, 1967.
[8] Typically these papers either ignore trapping or implicitly assume that collisions maintain a Maxwellian distribution.
[9] R. C. Davidson, J. Plasma Phys. **6**, 229 (1971).
[10] F. F. Chen, *Plasma Physics and Controlled Fusion* (Plenum Press, New York, 1984), p. 8.
[11] J. H. Malmberg, C. F. Driscoll, B. Beck, D. L. Eggleston, J. Fajans, K. Fine, X. P. Huang, and A. W. Hyatt, in *Nonneutral Plasma Physics,* edited by C. Roberson and C. Driscoll, AIP Conf. Proc. No. 175 (AIP, New York, 1988), p. 28.
[12] I. B. Bernstein, J. M. Greene, and M. D. Kruskal, Phys. Rev. **108**, 546 (1969).